Bias Dependence of Non-Fourier Heat Conduction in GaN HEMTs

Yang Shen

Department of Engineering Mechanics, School of Aerospace Engineering,
Tsinghua University

August 14, 2022

Overview

- Self-heating in GaN HEMTs can cause reliability issues and degrade the device performance. Being the result of Joule heating, self-heating is highly bias dependent.
- Previous studies on self-heating are mainly based on Fourier's law of heat conduction, the non-Fourier effects have not been studied quantitatively.
- We reexamined the bias dependence of self-heating in GaN HEMTs by TCAD and phonon Monte Carlo simulations, and developed a two-thermal-conductivity model which can address the bias dependence of phonon ballistic effects easily.

1. Introduction
   - Self-Heating in GaN HEMTs
   - Phonon Ballistic Transport in GaN HEMTs
2. Device Structure and Simulation Details
3. Results and Discussion
4. Conclusion

1. Introduction
   - Self-Heating in GaN HEMTs
   - Phonon Ballistic Transport in GaN HEMTs
2. Device Structure and Simulation Details
3. Results and Discussion
4. Conclusion

Thermal Issues in GaN HEMTs

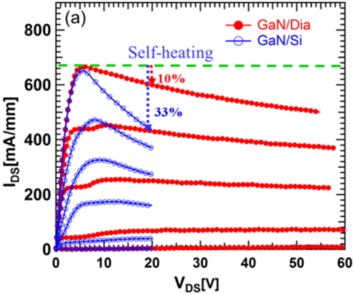

Figure 1: $I_{\mathrm{DS}} - V_{\mathrm{DS}}$ of GaN/Dia and GaN/Si HEMTs [1].

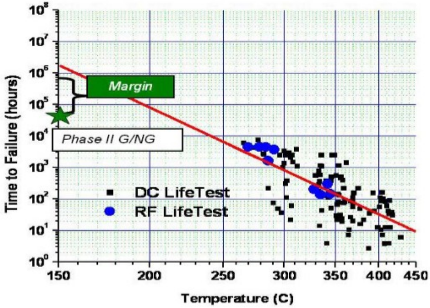

Figure 2: Mean time to failure (MTTF) for TriQuint GaN PAs [2].

The significant overheating within the devices largely degrades the electrical performance and shortens the device lifetime.

---

[1] K. Ranjan, S. Arulkumaran, G. Ng, *et al.*, "Investigation of self-heating effect on dc and rf performances in algan/gan hemts on cvd-diamond," *IEEE Journal of the Electron Devices Society*, vol. 7, pp. 1264–1269, 2019.

[2] M. Rosker, C. Bozada, H. Dietrich, *et al.*, "The darpa wide band gap semiconductors for rf applications (wbgs-rf) program: Phase ii results," *CS ManTech*, vol. 1, pp. 1–4, 2009.

Bias Dependence of Self-Heating

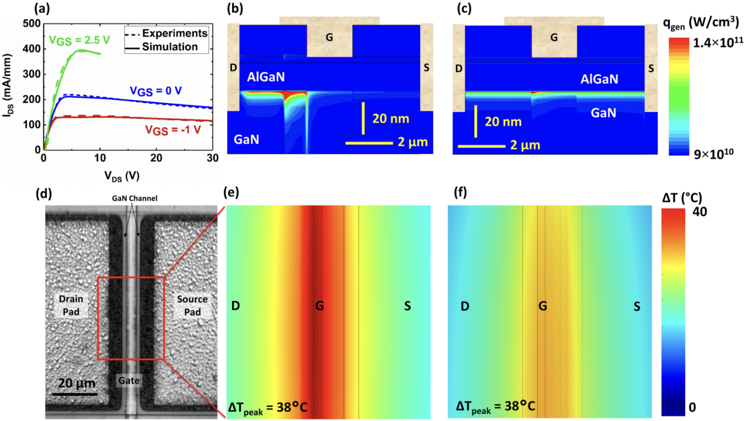

Figure 3: Bias dependent results for channel conditions with $V_{GS} = -1\,\text{V}$ and $V_{GS} = 2.5\,\text{V}$, respectively[3], $P_{diss} = 250\,\text{mW}$.

---

[3] B. Chatterjee, C. Dundar, T. E. Beechem, *et al.*, "Nanoscale electro-thermal interactions in AlGaN/GaN high electron mobility transistors," *Journal of Applied Physics*, vol. 127, no. 4, p. 044 502, 2020.

Bias Dependence of Self-Heating

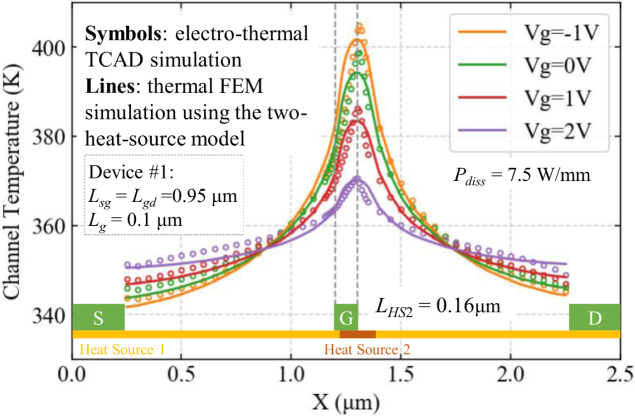

Figure 4: Temperature profiles across the channel at $P_{\text{diss}} = 7.5\,\text{W}/\text{mm}$ and the four different biases[4].

---

[4] X. Chen, S. Boumaiza, and L. Wei, "Modeling bias dependence of self-heating in gan hemts using two heat sources," *IEEE Transactions on Electron Devices*, vol. 67, no. 8, pp. 3082–3087, 2020.

1. Introduction
   - Self-Heating in GaN HEMTs
   - Phonon Ballistic Transport in GaN HEMTs
2. Device Structure and Simulation Details
3. Results and Discussion
4. Conclusion

Phonon Ballistic Transport

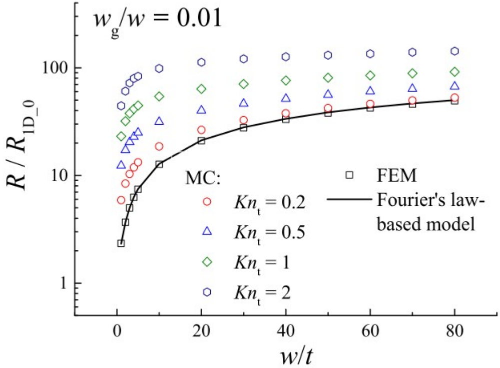

Figure 5: Dimensionless total thermal resistance as a function of w/t, with $w_g/w = 0.005$ and 0.01[5].

Phonon Ballistic Transport can significantly increase the thermal resistance.

---

[5] Y.-C. Hua, H.-L. Li, and B.-Y. Cao, "Thermal spreading resistance in ballistic-diffusive regime for GaN HEMTs," *IEEE Transactions on Electron Devices*, vol. 66, no. 8, pp. 3296–3301, 2019.

Multiscale Electrothermal Simulation[10]

The previous work considering the phonon transport in electrothermal simulations did not give some general and clear conclusions [6–9].

Also, the bias dependence of phonon ballsitic effects has not been studied quantitatively.

---

[6] N. Donmezer and S. Graham, “The impact of noncontinuum thermal transport on the temperature of algan/gan hfets,” *IEEE Transactions on Electron Devices*, vol. 61, no. 6, pp. 2041–2048, 2014.

[7] Q. Hao, H. Zhao, and Y. Xiao, “A hybrid simulation technique for electrothermal studies of two-dimensional GaN-on-SiC high electron mobility transistors,” *Journal of Applied Physics*, vol. 121, no. 20, p. 204 501, 2017.

[8] Q. Hao, H. Zhao, Y. Xiao, *et al.*, “Hybrid electrothermal simulation of a 3-d fin-shaped field-effect transistor based on GaN nanowires,” *IEEE Transactions on Electron Devices*, vol. 65, no. 3, pp. 921–927, 2018.

[9] B. Chatterjee, C. Dundar, T. E. Beechem, *et al.*, “Nanoscale electro-thermal interactions in AlGaN/GaN high electron mobility transistors,” *Journal of Applied Physics*, vol. 127, no. 4, p. 044 502, 2020.

[10] H. Rezgui, F. Nasri, G. Nastasi, *et al.*, “Design optimization of nanoscale electrothermal transport in 10 nm soi finfet technology node,” *Journal of Physics D: Applied Physics*, vol. 53, no. 49, p. 495 103, 2020.

This Work

Motivation

- Reexamine the bias dependence of self-heating in GaN HEMTs with the consideraton of phonon ballistic transport.

This Work

- TCAD and Monte Carlo simulations were conducted to study the self-heating in GaN HEMTs. Based on the two-heat-source model, this work proposed a two-thermal-conductivity model to consider the bias dependence of phonon ballistic effects easily.

1. Introduction
2. Device Structure and Simulation Details
   - Device Structure and TCAD Setup
   - Phonon Monte Carlo Simulation
3. Results and Discussion
4. Conclusion

Device Structure[11]

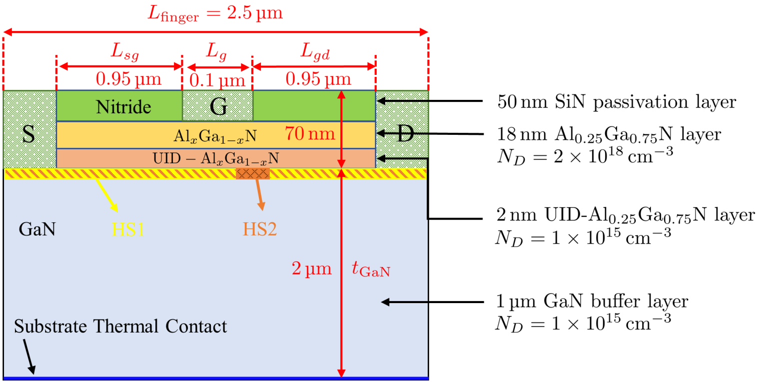

50 nm SiN passivation layer

18 nm $\text{Al}_{0.25}\text{Ga}_{0.75}\text{N}$ layer
$N_D = 2 \times 10^{18}\,\text{cm}^{-3}$

2 nm UID-$\text{Al}_{0.25}\text{Ga}_{0.75}\text{N}$ layer
$N_D = 1 \times 10^{15}\,\text{cm}^{-3}$

1 µm GaN buffer layer
$N_D = 1 \times 10^{15}\,\text{cm}^{-3}$

Figure 6: Schematic of the GaN HEMT for TCAD simulations.

---

[11] X. Chen, S. Boumaiza, and L. Wei, “Self-heating and equivalent channel temperature in short gate length gan hemts,” *IEEE transactions on electron devices*, vol. 66, no. 9, pp. 3748–3755, 2019.

Output Characteristics

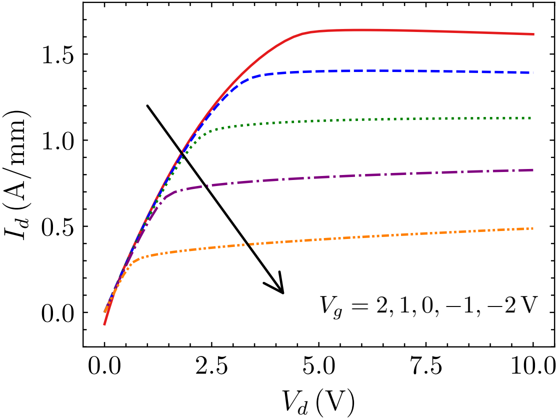

Figure 7: Output characteristics of the HEMT under V_g from -2 V to 2 V with an interval of 1 V.

1. Introduction
2. Device Structure and Simulation Details
   - Device Structure and TCAD Setup
   - Phonon Monte Carlo Simulation
3. Results and Discussion
4. Conclusion

Phonon Monte Carlo Simulation

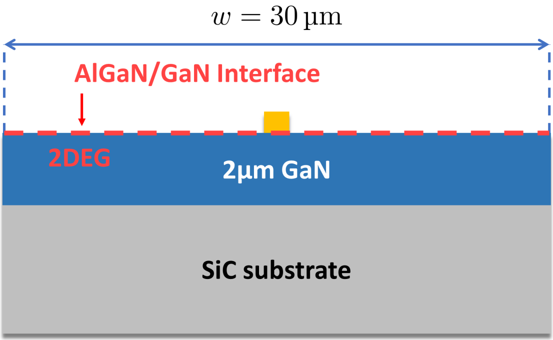

Figure 8: Schematic of GaN on SiC device for MC simulations.

Phonon Dispersion

- An isotropic sine-shaped phonon dispersion (Born-von Karman dispersion) is used.
- Longitudinal and transverse branches are not differentiated.

$$\omega(k) = \omega_\mathrm{m} \sin\left(\pi k / 2k_\mathrm{m}\right)$$

$$k_\mathrm{m} = \left(\frac{6\pi^2 N}{V}\right)^{1/3}, \; a = \pi / k_\mathrm{m}, \; \omega_\mathrm{m} = 2v_{0g}/a$$

Relaxation time

Matthiessen's rule[12]:

$$\tau^{-1} = \tau_{\mathrm{I}}^{-1} + \tau_{\mathrm{U}}^{-1} = A\omega^4 + B\omega^2 T \exp(-C/T)$$

Thermal conductivity fitting:

$$\mathscr{L}(A, B, C) = \sum_{T} \left\| \frac{1}{3} \sum_{p} \int_0^{\omega_{\mathrm{m}}} C_\omega v_\omega l_\omega \mathrm{d}\omega - k_{\mathrm{exp}} \right\|^2$$

$$C(\omega, p) = \hbar\omega D(\omega, p) \frac{\partial f^{\mathrm{m}}}{\partial T} = \hbar\omega \frac{\kappa^2}{2\pi^2 \left| v_g \right|} \frac{\hbar\omega e^{\frac{\hbar\omega}{Tk_B}}}{T^2 k_B \left(e^{\frac{\hbar\omega}{Tk_B}} - 1 \right)^2}$$

---

[12] G. Chen, *Nanoscale energy transport and conversion: a parallel treatment of electrons, molecules, phonons, and photons*. Oxford university press, 2005.

Phonon Dispersion and Relaxation time

Table 1: Fitted phonon dispersion and scattering parameters[13].

Parameter (Unit)	GaN	SiC
$k_0\,(1 \times 10^9\,\mathrm{m}^{-1})$	10.94	8.94
$\omega_m\,(1 \times 10^{13}\,\mathrm{rad/s})$	3.50	7.12
$a_D\,(\text{Å})$	2.87	3.51
$A\,(1 \times 10^{-45}\,\mathrm{s}^3)$	5.26	1.00
$B\,(1 \times 10^{-19}\,\mathrm{s/K})$	1.10	0.596
$C\,(\mathrm{K})$	200	235.0

---

[13] Q. Hao, H. Zhao, and Y. Xiao, "A hybrid simulation technique for electrothermal studies of two-dimensional GaN-on-SiC high electron mobility transistors," *Journal of Applied Physics*, vol. 121, no. 20, p. 204 501, 2017.

Phonon Dispersion and Relaxation time

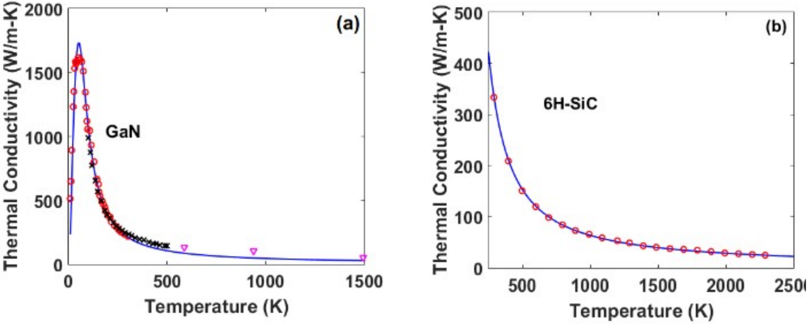

Figure 9: Thermal conductivity from model calculations (line), and from experiments (symbols)[14].

---

[14] Q. Hao, H. Zhao, and Y. Xiao, "Multi-length scale thermal simulations of gan-on-sichigh electron mobility transistors," in *MultiscaleThermal Transport in Energy Systems*, Nova Science Publishers, 2016.

Interface Phonon Transport

Based on diffuse mismatch model (DMM), phonons are diffusively transmitted or reflected by an interface.

The frequency-dependent phonon transmissivity from material 1 to 2 is given as

$$T_{12}(\omega) = \frac{\sum_p v_{2,g,p}(\omega) D_{2,p}(\omega)}{\sum_p v_{1,g,p}(\omega) D_{1,p}(\omega) + \sum_p v_{2,g,p}(\omega) D_{2,p}(\omega)}$$

The thermal boundary resistance (TBR) of GaN/SiC calculated by MC is 16 $\mathrm{m^2\,K/GW}$, which is in the same range of the experiments 5 $\mathrm{m^2\,K/GW}$–20 $\mathrm{m^2\,K/GW}$.

Bias-Dependent Heat Generation

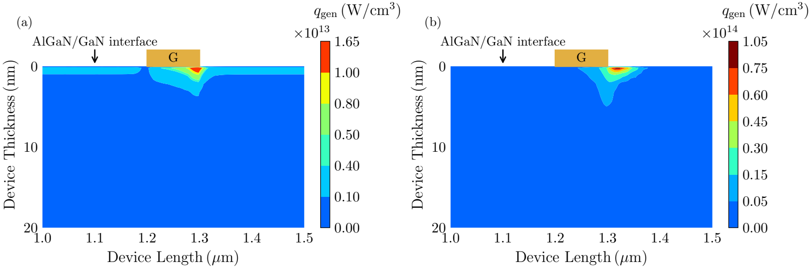

(a) $V_g = 2\,\text{V}$, $V_d = 5.5\,\text{V}$ (b) $V_g = -1\,\text{V}$, $V_d = 9.5\,\text{V}$

Figure 10: The total power dissipation level for the two bias condions, $P = 7.5\,\text{W/mm}$.

Two-Heat-Source Model

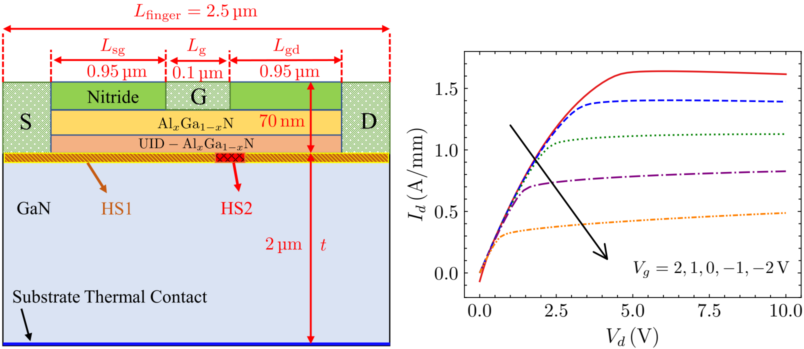

Figure 11: Schematic of the two-heat-source model.

$$\begin{cases} P_1 = I_{\text{d}} V_{\text{d}},\, P_2 = 0, & V_{\text{d}} \le V_{\text{dsat}} \\ P_1 = I_{\text{d}} V_{\text{dsat}},\, P_2 = I_{\text{d}}\left(V_{\text{d}} - V_{\text{dsat}}\right), & V_{\text{d}} > V_{\text{dsat}} \end{cases}$$

1 Introduction

2 Device Structure and Simulation Details

3 Results and Discussion
- Bias-Dependent Heat Generation
- Temperature Distribution in the HEMT
- Thermal Resistance of GaN Buffer Layer
- Two-Thermal-Conductivity Model

4 Conclusion

Temperature Distribution

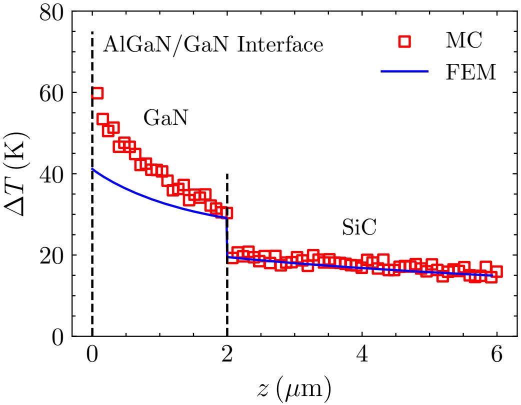

Figure 12: Temperature rise along the thickness direction at drain-side gate edge, $V_g = 2\,\mathrm{V}$, $V_d = 4\,\mathrm{V}$.

Phonon ballistic effects mainly exist in GaN buffer layer.

Bias-Dependent Channel Temperature

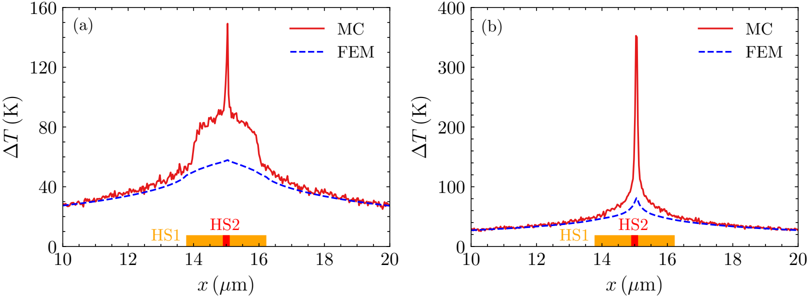

(a) $V_g = 2\,\text{V}$, $V_d = 5\,\text{V}$ (b) $V_g = -1\,\text{V}$, $V_d = 9.5\,\text{V}$

Figure 13: Temperature rise along the AlGaN/GaN interface, $P_{\text{diss}} = 7.5\,\text{W/mm}$.

Bias-Dependent Channel Temperature

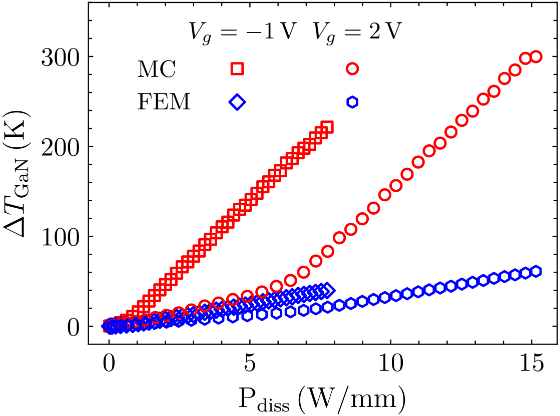

Figure 14: Maximum temperature rise in GaN layer at different biases predicted by MC and FEM.

1. Introduction

2. Device Structure and Simulation Details

3. Results and Discussion
   - Bias-Dependent Heat Generation
   - Temperature Distribution in the HEMT
   - Thermal Resistance of GaN Buffer Layer
   - Two-Thermal-Conductivity Model

4. Conclusion

Differential Thermal Resistance of GaN Layer

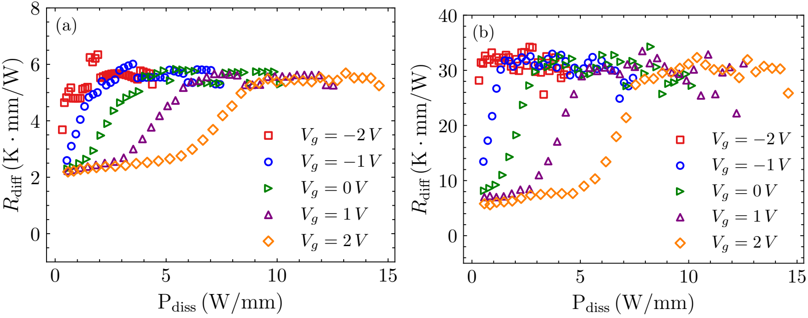

(a) FEM

(b) MC

Figure 15: Differential thermal resistance R_{diff}, computed as the derivative of ΔT_{GaN} versus P_{diss}

Thermal Resistance of GaN Layer

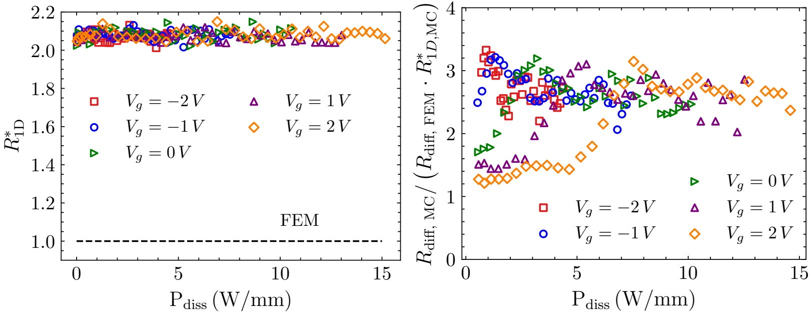

(a) 1D thermal resistance (b) thermal resistance ratio

Figure 16: Thermal resistance of the GaN layer.

The cross-plane ballistic effect stays nearly constant at different biases, whereas the ballistic effect with the heat generation region size comparable with MFP is highly bias-dependent.

1. Introduction
2. Device Structure and Simulation Details
3. Results and Discussion
    - Bias-Dependent Heat Generation
    - Temperature Distribution in the HEMT
    - Thermal Resistance of GaN Buffer Layer
    - Two-Thermal-Conductivity Model
4. Conclusion

Effective Thermal Conductivity Model[15,16]

The degradation of the effective thermal conductivity is caused by the suppression of mean free paths of phonons,

$$k_{\text{eff}} = \frac{1}{3}\sum_j \int_0^{\omega_j} \hbar\omega \frac{\partial f_0}{\partial T} \mathrm{DOS}_j(\omega) v_{g,\omega,j} l_{m,j} d\omega$$

Where

$$l_{m,j} = \frac{l_{0,j}}{\left(1 + \frac{2}{3}Kn_{t\_\omega,j}\right)\left(1 + A_w\left(\frac{w_g}{w}, \frac{w}{t}\right)Kn_{w\_\omega,j}\right) r_t r_{wg}}$$

---

[15] Y.-C. Hua, H.-L. Li, and B.-Y. Cao, "Thermal spreading resistance in ballistic-diffusive regime for GaN HEMTs," *IEEE Transactions on Electron Devices*, vol. 66, no. 8, pp. 3296–3301, 2019.

[16] Y. Shen, Y.-C. Hua, H.-L. Li, *et al.*, "Spectral thermal spreading resistance of wide-bandgap semiconductors in ballistic-diffusive regime," *IEEE Transactions on Electron Devices*, vol. 69, no. 6, pp. 3047–3054, 2022.

Two-Thermal-Conductivity Model

$k_1 = 94.47\,\mathrm{W/mK}, k_2 = 47.38\,\mathrm{W/mK}$

$$T_{max} = T_0 + \frac{k_{\mathrm{bulk}}}{k_1} P_1 R_1 + \frac{k_{\mathrm{bulk}}}{k_2} P_2 R_2$$

Where

$$\begin{cases} P_1 = I_{\mathrm{d}} V_{\mathrm{d}}, P_2 = 0, & V_{\mathrm{d}} \leq V_{\mathrm{dsat}} \\ P_1 = I_{\mathrm{d}} V_{\mathrm{dsat}}, P_2 = I_{\mathrm{d}} \left(V_{\mathrm{d}} - V_{\mathrm{dsat}} \right), & V_{\mathrm{d}} > V_{\mathrm{dsat}} \end{cases}$$

R_1 and R_2 are the thermal resistance seen by HS1 and HS2 of the GaN layer, respectively. T_0 is the maximum temperature of bottom of the GaN layer predicted by FEM.

Validation of the Model

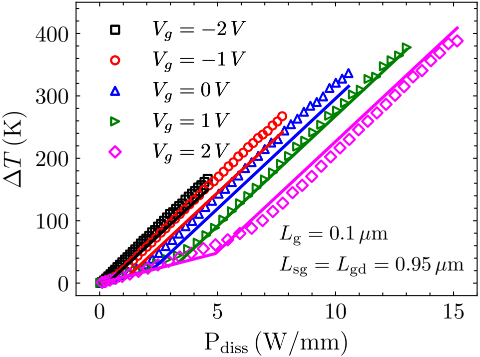

Figure 17: Maximum channel temperature rise versus total power dissipation P_{diss} at different biases.

Devices with Different Geometries

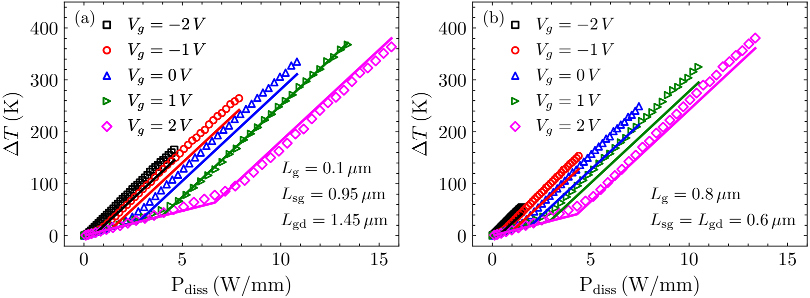

Figure 18: Maximum channel temperature rise versus total power dissipation P_{diss} at different biases.

1. Introduction
2. Device Structure and Simulation Details
3. Results and Discussion
4. Conclusion

Conclusion

- Phonon ballistic effect can significantly increase the thermal resistance of the GaN layer and is highly bias-dependent.
- The cross-plane ballistic effect stays nearly constant at different biases. Whereas with the concentration of heat generation, the ballistic effect with the heat generation size comparable with MFP increases significantly.
- Based on the two-heat-source model, we proposed a two-thermal-conductivity model which provides a simple approach to incorporate the phonon ballistic effect with FEM without the need for complicated multiscale electrothermal simulations.

Thank You!